JOURNAL OF GEOPHYSICAL RESEARCH: SPACE PHYSICS, VOL. 118, 5403–5414, doi:10.1002/jgra.50504, 2013

Spatio-temporal entropy analysis of the magnetic field to help magnetic cloud characterization

A. Ojeda G.,[1,2] O. Mendes,[1] M. A. Calzadilla,[2] and M. O. Domingues[3]

Received 15 January 2013; revised 11 July 2013; accepted 10 August 2013; published 5 September 2013.

[1] The aim of this work is to create a methodology to characterize the dynamics of magnetic clouds (MCs) from signals measured by satellites in the interplanetary medium. We have tested spatio-temporal entropy (STE) technique to study 41 MCs identified by other authors, where the plasma sheath region has been identified. The STE was implemented in Visual Recurrence Analysis software to quantify the order in the recurrence plot. Some tests using synthetic time series were performed to validate the method. In particular, we worked with interplanetary magnetic field (IMF) components B_x, B_y, B_z of 16 s. Time windows from March 1998 to December 2003 for some MCs were selected. We found higher STE values in the sheaths and 0 STE values in some of the three components in most of the MCs (30 among 41 events). The trend is the principal cause of the lower STE values in the MCs. Also, MCs have magnetic field more structured than sheath and quiet solar wind. We have done a test considering the magnetic components of a cylindrically symmetric force-free field constructed analytically, with the result of 0 STE value. It agrees with the physical assumption of finding 0 STE values when studying experimental data in MC periods. The new feature just examined here adds to the usual features, as described in Burlaga et al. (1981), for the characterization of MCs. The STE calculation can be an auxiliary objective tool to identify flux ropes associated with MCs, mainly during events with no available plasma data but only with IMF.

Citation: Ojeda G., A., O. Mendes, M. A. Calzadilla, and M. O. Domingues (2013), Spatio-temporal entropy analysis of the magnetic field to help magnetic cloud characterization, *J. Geophys. Res. Space Physics*, *118*, 5403–5414, doi:10.1002/jgra.50504.

1. Introduction

[2] The term magnetic cloud (MC) has been used to characterize an interplanetary coronal mass ejection (ICME) that presents a specific configuration, in which the magnetic field strength is higher than average interplanetary magnetic field (IMF), the magnetic field direction rotates smoothly through a large angle, and the proton temperature is low [*Burlaga et al.*, 1981; *Klein and Burlaga*, 1982; *Gosling*, 1990]. Typically, a flux rope ejected from the Sun described the magnetic configuration of a MC. The MCs are observed in a clear way when the spacecraft crosses the magnetic field structure close by its center [*Schwenn*, 2006]. In situ measurements are limited to the spacecraft trajectory crossing the incoming ICME. Therefore, one needs to rely on modeling evaluation in order to derive the global magnetic structure from available local measurements [*Démoulin and Dasso*, 2009]. Due to MCs moving faster than the surrounding solar wind (SW), plasmas and magnetic field typically accumulate in front of it, creating a preceding disturbed sheath.

[3] In *Ojeda et al.* [2005], a study considering 20 MCs, 17 non-MC ICMEs, and 20 time series of equivalent time duration of quiet SW was done. The IMF B_z and solar wind V_x components in a time interval of 48 h before each MC were analyzed. Under MC conditions, a feature was identified that the component B_z of the IMF has the tendency to present lower spatio-temporal entropy (name given by Eugene Kononov's Visual Recurrence Analysis (VRA) software, not to be confused with spatio-temporal entropy image (STEI) [*Ma and Zhang*, 2001]) values than the B_z in other cases, such as in non-MC ICMEs and during quiet SW. This behavior seems to be very interesting under a physical point of view. Thus, in this work a more detailed study of the spatio-temporal entropy (STE) in MCs is carried out. The analyses are expanded to study the three magnetic components (B_x, B_y, and B_z) using more complete data set. The aim of this work is to validate the STE calculation technique as a useful tool to identify features of the MCs. A proposed approach to study the MCs by analyzing the time series of interplanetary magnetic field (IMF) is presented.

[1] Division of Space Geophysics, National Institute for Space Research, São José dos Campos SP, Brazil.

[2] Department of Space Geophysics, Institute of Geophysics and Astronomy, Havana, Cuba.

[3] Associate Laboratory of Applied Computing and Mathematics, National Institute for Space Research, São José dos Campos SP, Brazil.

Corresponding author: Arian Ojeda González, National Institute for Space Research, Division of Space Geophysics, Av. dos Astronautas, 1758 - Jd. Granja, São José dos Campos SP, Brazil - CEP 12227-010. (ojeda.gonzalez.a@gmail.com)

2169-9380/13/10.1002/jgra.50504

[4] The content is organized as follows. In section 2 a review on the theoretical and observational aspects of the interplanetary MCs is presented. In section 3 the data set used is described. In section 4 a STE methodology for analyses is established. In section 5 we compare STE values for time series corresponding to the MCs and the sheaths identified by *Huttunen et al.* [2005]. Finally, in section 6 the conclusions are done. In Appendices, information on the tool is presented. Appendix A shows a review on the tool in the VRA software. Appendix B shows the methods for calculating the entropy in the recurrence plot.

2. Magnetic Clouds

[5] The pioneer studies on plasma clouds emitted by the Sun were developed in about the 1950s [*Morrison*, 1954; *Cocconi et al.*, 1958; *Piddington*, 1958]. However, the definition and the term of "magnetic cloud" were presented for the first time in the work of *Burlaga et al.* [1981]. Nowadays the specific signatures which have to be necessarily fulfilled are the following: (1) smooth rotation in $\vec{B}$ with low variance; (2) low proton temperature; and (3) low plasma β, which is the ratio of the plasma pressure, $p = nk_BT$, to the magnetic pressure, $p_{mag} = B^2/2\mu_0$ where n is number density, k_B Boltzmann constant, T temperature, B magnetic field, and μ_0 magnetic permeability of the free space.

[6] Initial studies to analyze the three-dimensional configuration of the magnetic field of these phenomena have been developed by *Burlaga et al.* [1981]. The minimum variance analysis (MVA) was used as a method to identify and describe planar magnetic field configuration associated with thin current sheets in the SW [*Burlaga and Klein*, 1980] and planetary magnetospheres [*Lepping and Behannon*, 1979]. *Burlaga et al.* [1981] used MVA to analyze the magnetic field configuration in a MC observed with four spacecraft: Voyager 1 and 2, IMP 8, and Helios 2. They concluded that MC could be represented as a magnetic cylinder whose axis lies close in the equatorial plane, marking an angle of nearly 90° with respect to the radial direction.

[7] Considering a cylindrical geometry for MCs, the MVA [*Sonnerup and Cahill*, 1967] became a useful tool to calculate the direction of the cloud axis. *Klein and Burlaga* [1982] identified 45 events in the period between 1967 and 1978, where the latitude and longitude of the clouds axis were calculated. The results of *Burlaga et al.* [1981] also were consistent with other configurations. *Ivanov and Harshiladze* [1984] created a mathematical formulation using a cloud configuration as an oblate ellipsoidal. To understand how the magnetic field configuration evolves in the SW may be necessary for the correct interpretation of the field structure in MC [*Burlaga and Behannon*, 1982].

[8] *Goldstein* [1983] considered a force-free configuration in the search for a stable topology of the MCs. *Marubashi* [1986] studied interplanetary magnetic field data from the Pioneer Venus orbiter (PVO) between December 1978 and May 1984 in search of interplanetary magnetic flux ropes near the Venus orbit. As a result, 26 well-defined flux ropes were found which have characteristics similar to those of flux ropes observed near Earth. In one case, where the Sun, Venus, and Earth were closely aligned, an almost identical structure was observed by the PVO and the Earth-orbiting spacecraft with a time delay of about 36 h. This observation provides evidence that the structures of interplanetary magnetic flux ropes are maintained during propagation at least from 0.72 AU (astronomical unit (AU): the average distance from the Earth to the Sun; 1 AU = 93 million miles or 149.6 million km) to 1 AU. A simple solution for a cylindrically symmetric force-free field with constant alpha was studied by *Lundquist* [1950] and mentioned also in *Lundquist* [1951]. *Burlaga* [1988] studied the above solution with constant alpha to describe the types of signatures observed in the SW at 1 AU when MCs move past a spacecraft.

Table 1. Summary of Seven Previous Studies That Identified MCs Before 2003[a]

Paper[b]	Period	T_t (Years)	Spacf	MC
1	1965–1993	28	OMNI	67
2	Dec/1974–Jul/1981	6.7	Helios 1/2	45
3	1979–1988	10	Pioneer	61
4	Feb/1998–Jul/2001	3.5	ACE	56
5	1995–2002	8	WIND	71
6	1997–2003	7	WIND/ACE	73
7	2000–2003	4	WIND/ACE	35

[a]Adapted from *Huttunen et al.* [2005].
[b]In column 1: 1, *Bothmer and Rust* [1997]; 2, *Bothmer and Schwenn* [1998]; 3, *Mulligan et al.* [1998]; 4, *Lynch et al.* [2003]; 5, *Wu et al.* [2003]; 6, *Huttunen et al.* [2005]; 7, *Nieves-Chinchilla et al.* [2005].

[9] In order to find plasma beta values significantly lower than 1 to identify MCs, spacecraft measurements of magnetic field and plasma are required. Sometimes the temperature and density data on spacecraft have many gaps during periods in which the plasma instruments are saturated as a result of intense particle fluxes (for example, Bastille Day in the ACE spacecraft). If this condition occurs, it becomes impossible to calculate the plasma beta, but it is still possible to detect the MC using magnetometer data [e.g., *Huttunen et al.*, 2005; *Nieves-Chinchilla et al.*, 2005]. Here is the contribution we intend to do with this work, showing an approach that could help to identify MCs, and it is proposed as a basis for an auxiliary analysis tool.

[10] The main contributions related to the identification of MCs are summarized in Table 1. It was adapted from *Huttunen et al.* [2005] and updated by us. We show in each column of this table the paper, the period of the investigation, the examination period (T_t), the spacecraft used (Spacf), and the number of MCs identified. *Bothmer and Rust* [1997], *Bothmer and Schwenn* [1998], and *Huttunen et al.* [2005] identified MCs based on the MVA method; *Mulligan et al.* [1998] identified and classified MCs using the visual inspection of the data; *Lynch et al.* [2003] and *Wu et al.*[2003, /WIND list] used the least-square fitting routine by *Lepping et al.* [1990], while *Nieves-Chinchilla et al.* [2005] studied all the MCs observed during the time interval 2000–2003 using the elliptical cross-section model [*Hidalgo*, 2003, 2005], where a distortion and expansion of the cross section of the cloud is included from first principles.

[11] From 1997 to 2003 in solar cycle 23, SW data were investigated by *Huttunen et al.* [2005] using the MVA method [*Sonnerup and Cahill*, 1967; *Bothmer and Schwenn*, 1998] to determine if they have flux-rope structures. They identified 73 MCs observed by the ACE and WIND spacecraft. In principle the axis of a MC can have any orientation with respect to the ecliptic plane [*Bothmer and Schwenn*,

1994; , 1998], identified by the azimuthal direction in the ecliptic, called ϕ_C, and the inclination relative to the ecliptic, called θ_C. With the MVA, the angles above can be calculated [*Bothmer and Schwenn*, 1998]. In order to classify MCs [*Huttunen et al.*, 2005, and references therein], eight flux-rope categories are often used, clustered as bipolar MCs (low inclination, and flux-rope type SWN, SEN, NES, or NWS), $\theta_C \leq 45°$, and unipolar MCs (high inclination, and flux-rope type WNE, ESW, ENW, or WSE), $\theta_C > 45°$, where the meanings are S for south, N for North, W for west, and E for east.

[12] Huttunen and collaborators have also included seven cloud candidate events for which either the fitting with MVA was not successful (e.g., the eigenvalue ratio < 2 or the directional change less than 30°) or there were large values of beta throughout the event. In their study, the criterion to identify a MC was based on the smoothness of the rotation in the magnetic field direction confined to one plane. Additionally, they required that a MC must have the average values of the plasma beta less than 0.5, the maximum value of the magnetic field at least 8 nT, and the duration at least 6 h. The last two criteria have been created with the objective of excluding "small and weak MCs." All selected events were investigated by analyzing 1 h magnetic field data with the minimum variance analysis (MVA), where MCs are identified from the smooth rotation of the magnetic field vector in the plane of the maximum variance [*Klein and Burlaga*, 1982]. For MCs with durations of 12 h or less *Huttunen et al.* [2005] performed MVA using 5 min (WIND) or 4 min (ACE) averaged data.

3. IMF Data Set

[13] The IMF data set used in this work comprises measurements obtained by the ACE satellite. The ACE spacecraft is in orbit around $L1$ from 1997 [*Smith et al.*, 1998]. Where the Lagrangean point $L1$ is a gravitational equilibrium point between the Sun and Earth at about 1.5 million km from Earth and 148.5 million km from the Sun. On board of ACE a total of 10 instruments were launched toward $L1$ [*McComas et al.*, 1998], but in this work only the Magnetic Field Experiment (MAG) is used. The MAG on board ACE consists of twin vector fluxgate magnetometers to measure the IMF [*Smith et al.*, 1998]. The data (http://www.srl.caltech.edu/ACE/ASC/level2/index.html) contain time averages of the magnetic field over time periods 1 s, 16 s, 4 min, hourly, daily, and 27 days (1 Bartels rotation). In this work, IMF components (B_x, B_y, B_z) with time resolution of 16 s in GSM coordinate systems are used.

[14] We only work with 41 of 73 MCs identified by *Huttunen et al.* [2005] from March 1998 to December 2003, where the MCs were preceded by the plasma sheaths. We are interested in comparing these two regions when they have been well identified. The 41 events in chronological order are shown in Table 2. The columns from the left to the right give a numeration of the events, year, shock time (UT), MC start time (UT), and MC end time (UT), respectively.

Table 2. Solar Wind Data Studied [From *Huttunen et al.*, 2005]

No.	Year	Shock	UT	Start	UT	Stop	UT
01	1998	06 Jan	13:19	07 Jan	03:00	08 Jan	09:00
02		03 Feb	13:09	04 Feb	05:00	05 Feb	14:00
03		04 Mar	11:03	04 Mar	15:00	05 Mar	21:00
04		01 May	21:11	02 May	12:00	03 May	17:00
05		13 Jun	18:25	14 Jun	02:00	14 Jun	24:00
06		19 Aug	05:30	20 Aug	08:00	21 Aug	18:00
07		24 Sep	23:15	25 Sep	08:00	26 Sep	12:00
08		18 Oct	19:00	19 Oct	04:00	20 Oct	06:00
09		08 Nov	04:20	08 Nov	23:00	10 Nov	01:00
10		13 Nov	00:53	13 Nov	04:00	14 Nov	06:00
11	1999	18 Feb	02:08	18 Feb	14:00	19 Feb	11:00
12		16 Apr	10:47	16 Apr	20:00	17 Apr	18:00
13		08 Aug	17:45	09 Aug	10:00	10 Aug	14:00
14	2000	11 Feb	23:23	12 Feb	12:00	12 Feb	24:00
15		20 Feb	20:57	21 Feb	14:00	22 Feb	12:00
16		11 Jul	11:22	11 Jul	23:00	13 Jul	02:00
17		13 Jul	09:11	13 Jul	15:00	13 Jul	24:00
18		15 Jul	14:18	15 Jul	19:00	16 Jul	12:00
19		28 Jul	05:53	28 Jul	18:00	29 Jul	10:00
20		10 Aug	04:07	10 Aug	20:00	11 Aug	08:00
21		11 Aug	18:19	12 Aug	05:00	13 Aug	02:00
22		17 Sep	17:00	17 Sep	23:00	18 Sep	14:00
23		02 Oct	23:58	03 Oct	15:00	04 Oct	14:00
24		12 Oct	21:36	13 Oct	17:00	14 Oct	13:00
25		28 Oct	09:01	28 Oct	24:00	29 Oct	23:00
26		06 Nov	09:08	06 Nov	22:00	07 Nov	15:00
27	2001	19 Mar	10:12	19 Mar	22:00	21 Mar	23:00
28		27 Mar	17:02	27 Mar	22:00	28 Mar	05:00
29		11 Apr	15:18	12 Apr	10:00	13 Apr	06:00
30		21 Apr	15:06	21 Apr	23:00	22 Apr	24:00
31		28 Apr	04:31	28 Apr	24:00	29 Apr	13:00
32		27 May	14:17	28 May	11:00	29 May	06:00
33		31 Oct	12:53	31 Oct	22:00	02 Nov	04:00
34	2002	23 Mar	10:53	24 Mar	10:00	25 Mar	12:00
35		17 Apr	10:20	17 Apr	24:00	19 Apr	01:00
36		18 May	19:44	19 May	04:00	19 May	22:00
37		01 Aug	23:10	02 Aug	06:00	02 Aug	22:00
38		30 Sep	07:55	30 Sep	23:00	01 Oct	15:00
39	2003	20 Mar	04:20	20 Mar	13:00	20 Mar	22:00
40		17 Aug	13:41	18 Aug	06:00	19 Aug	11:00
41		20 Nov	07:27	20 Nov	11:00	21 Nov	01:00

4. Methodology Using STE Analysis

[15] Based on the description of MCs, a proper statistical tool can be used to identify their typical features. The STE analysis was chosen to establish a methodology. The STE analysis consists of a tool that compares the distribution of distances between all pairs of vectors in the reconstructed state space with that of distances between different orbits evolving in time. In this context, the terms "state space" and "orbits" are concepts of the theory of chaotic dynamical systems. State space reconstruction is the first step in nonlinear time series analysis of data from chaotic systems including estimation of invariants and prediction. Dynamical regimes, such as a resting state or periodic oscillation, correspond to geometric objects, such as a point or a closed curve, in the phase space. Evolution of a dynamical system corresponds to a trajectory (or an orbit) in the phase space. Different initial states result in different trajectories. In the recurrence plot (RP) a one-dimensional time series from a data file is expanded into a higher-dimensional space, in which the dynamic of the underlying generator takes place. The concept of state space and orbit are also valid in the RP and in the subsequent calculation of the STE. The STE results identify in a certain objective way the characteristics of a physical process present in a time measurement data set.

[16] The VRA software provides resources to investigate this promising approach immediately. The recurrence plot

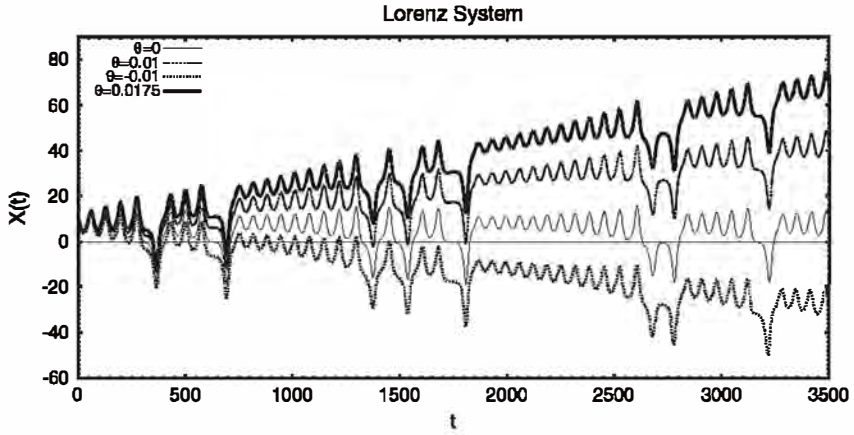

Figure 1. Time series plot of Lorenz data file included in VRA (case with $\theta = 0$). Series rotated about origin ($\theta = -0.01$ rad, $\theta = 0.01$ rad, $\theta = 0.0175$ rad) and the three resulting series also plotted. After that, we calculate the STE of each time series.

has been used. For more details, the information on it is presented in Appendix A (recurrence plot) and Appendix B (entropy).

[17] In this section, the purpose is to show the variation of STE values after processing carried out in some synthetic time series file included in VRA software. The methodology to study synthetic time series will be implemented, with the purpose to be applied to analyze IMF data set.

4.1. STE Variations Versus Trend Angle

[18] From an intuitive point of view, a time series is said to be stationary if there is no trend and no systematic change in variance and if strictly periodic variations have been removed [*Chatfield*, 2003]. Trend estimation is a statistical technique that could be an aid in the interpretation of data [*Chatfield*, 2003]. When a time series related to measurements of a process is treated, trend estimation can be used to make and justify statements about tendencies in the data. Given a set of data and the desire to produce some kind of function fitted through those data, the simplest function to fit is a straight line (using least-squares fit). If there is no global trend in time series, the angle ("trend angle") between the straight line and the positive x axis must be 0.

[19] We have calculated the STE value for each temporal series with embedding dimension and time delay equal to 1, respectively. It may be noticed that STE value changes for different embedding parameters. For example, for Lorenz attractor (Lorenz data file included in VRA), STE is near its minimum when the correct embedding is used (dimension = 3, time delay = 16 to this particular data file). This and other results suggest that STE can be used to determine the optimal embedding parameters, which is not the aim in this work. We selected the same embedding and time delay, equal to 1, to maintain equivalence in the calculation of STE among all series in order to compare the results, because our hypothesis is that this tool (STE) could be useful in a computational implementation to characterize MCs or use as a new property of MCs.

[20] With the VRA software a group of synthetic time series were included. It included a variety of time series with different properties, i.e., periodic, random, and with noises and chaos, respectively. A data set of time series, Lorenz, sine, and white noise are used as test cases to validate the STE calculation.

[21] Figure 1 shows a time series plot of Lorenz data file included in VRA software. We gave trends to the series through angular rotations about the origin. The time series have 3500 data records, and they were rotated about the origin, angles of 0, –0.01, 0.01, and 0.0175 rad, respectively. The STE values have been calculated for each time series, and the results are shown in Table 3, row 2.

[22] We follow the same idea to cause a trend in time series for other cases, sine and white noise data file also included in VRA software. The results have been included in rows 3 and 4 in Table 3. In periodic time series (sine data file) the STE value is always 0 independent of increasing trend. In the other two cases if time series trend increases, then the STE values decrease (see rows 2 and 4 in Table 3). We are doing those kinds of tests because we know that inside MCs the trend of IMF components increases, and we are interested in knowing how it could affect STE values.

[23] To go on with the above idea, it is good to know that the time series of the first difference is often enough to convert series with a trend into a stationary time series. The first-order differences of time series values $x_1, x_2, x_3, \cdots, x_N$ are given by a new series $y_1, y_2, \cdots, y_{N-1}$, where $y_{N-1} = x_N - x_{N-1}$. The operation $y_t = x_t - x_{t-1} = \nabla x_t$ is called the first difference, and ∇ is the difference operator [*Chatfield*, 2003].

[24] Our interest is to study variations in the STE values when first-order differences are applied on stationary time series. In time series studied previously (Lorenz, sine, and white noise), new time series from the first-order differences have been constructed. After that, we calculated STE values of each time series and the results were compared with the

Table 3. STE Values Related to Trends for Three Time Series With Data File Included in VRA 4.7

Series/angle (rad)	0	–0.01	0.01	0.0175
STE (Lorenz)	73%	30%	29%	0%
STE (sine)	0%	0%	0%	0%
STE (white noise)	80%	34%	34%	3%

Table 4. STE Values Related to the First-Order Differences in Time Series

Series	Untransformed	First-Order Differences
STE (Lorenz)	73%	75%
STE (sine)	0%	0%
STE (white noise)	80%	82%

original series (nondifferentiated or untransformed) shown in Table 4. The STE values are similar in both of them, i.e., for transformed (first-order differences) and untransformed time series. Thus, if the time series has no trend, then the nonlinear delicate structures are not destroyed.

[25] The STE value is low and may tend to 0 in any time series with trend. If there is a trend in the time series, it could be removed by differencing the original time series before calculating the STE. However, taking the first differences may interfere with the delicate nonlinear structure in the time series (if there is any). Thus, STE values are calculated on the untransformed series and then in the transformed series, where the first-order differences are applied. This is done on a trial basis after calculating STE values of the original series.

4.2. Variations of STE Values Given by Time Series Size

[26] The calculation of the STE with the VRA software version 4.7 cannot be made in time series with size larger than $\sim$ 5000 points because the STE has a rapid decrease to 0. It seems to be a limitation of the software by some reason not explained in its tutorial. To exemplify the previous statement, synthetic series have been created using a pseudorandom number generator producing values in the range 0 to 1. In Figure 2 (top), an example with 3000 points is shown. In this time series a STE value of 86% was calculated. Figure 2 (bottom) shows the plot of STE values versus length(X(t)) of 18 time series constructed as shown in the top panel. The STE values decrease in time series with a length larger than $\sim$ 4000 points. When using the VRA software someone must take into account this identified limitation in the extension (length) of the data under analysis.

4.3. Scheme to Study STE Values in IMF Components

[27] Figure 3 shows the scheme that will be used to characterize MCs. From the 73 that have been identified by *Huttunen et al.* [2005] from March 1998 to December 2003, 41 are selected, the cases where the plasma sheath is also identified. For both regions, time series of IMF components with time resolution of 16 s, in GSM coordinates system, are selected.

[28] Using VRA software, the data without transformations are processed. Also the same data before using the software are transformed. The aim of the transformations is to eliminate the trend and noises, respectively. The trends are eliminated with two techniques, e.g., doing first-order differences at time series and a rotation about the origin; in the beginning of this section both techniques were explained. To filter the white noise, a Gaussian filter can be used, e.g., *Mendes et al.* [2006]. Inside the VRA software the RPs are generated and the STE values are calculated.

[29] Using a simple solution for a cylindrically symmetric force-free field with constant alpha [*Burlaga*, 1988], time series were constructed. For a physical evaluation, the STE values are calculated. Finally, with the results, the MCs are characterized.

5. Results and Discussion

[30] The STE values for the 41 MC events are shown in Figure 4. At the top, the STE values calculated from the three IMF components, B_x, B_y, and B_z, plotted respectively as circles, plus symbols, and cross symbols, correspond to MCs. The bottom plot is the same as that above but is for the sheath regions. The STE values of the 246 time series ($3 \times (41\text{MCs} + 41\text{Shts}) = 246$) were plotted in chronological order as shown in Table 2 column 1. Some MCs do not have STE values close to 0 in the three components simultaneously. Then, it is possible to find components with perfect structuredness (low STE) and absence of structure (high STE) in the same MC.

[31] If STE values between the same components for the plasma sheath and the MC regions are compared (e.g., B_x-sheath (STE = 56%) with B_x-cloud (STE = 0%) in event number 1), then in 5/41 (3/41) of the cases, in the B_x (B_y, B_z) component(s), the STE value in the MC is larger than at its plasma sheath region, respectively. These are few cases and show a clear tendency to decrease the STE value within the

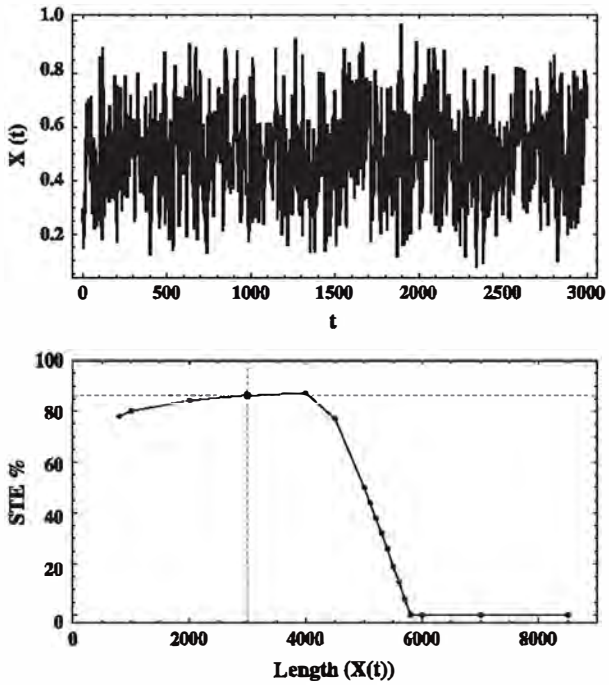

Figure 2. (top) X(t) versus t is plotted, where X(t) is a synthetic series created using a pseudorandom number generator producing values in the range 0 to 1. A simple moving average is applied to show the graph. The time series of pseudorandom number has a recurrence plot similar to that shown in Figure A1 (bottom), and the STE value of this time series is 86%. (bottom) The STE values versus length (X(t)) of time series constructed. These values decrease in time series with a length larger than $\sim$ 4000 points.